Journal of Applied Physics ARTICLE scitation.org/journal/jap

Deep levels related to the carbon antisite–vacancy pair in 4H-SiC

Cite as: J. Appl. Phys. **130**, 065703 (2021); doi: 10.1063/5.0059953
Submitted: 14 June 2021 · Accepted: 27 July 2021 ·
Published Online: 11 August 2021

View Online Export Citation CrossMark

Hiroki Nakane,[1] Masashi Kato,[1,2] Yutaro Ohkouchi,[1] Xuan Thang Trinh,[3,a)] Ivan G. Ivanov,[3] Takeshi Ohshima,[4] and Nguyen Tien Son[3,b)]

AFFILIATIONS

[1]Department of Engineering Physics, Electronics and Mechanics, Nagoya Institute of Technology, Gokiso, Showa, Nagoya 466-8555, Japan
[2]Frontier Research Institute for Materials Science, Nagoya Institute of Technology, Nagoya 466-8555, Japan
[3]Department of Physics, Chemistry and Biology, Linköping University, SE-581 83 Linköping, Sweden
[4]National Institutes for Quantum and Radiological Science and Technology, 1233 Watanuki, Takasaki, Gunma 370-1292, Japan

[a)]**Present address:** Research Laboratories of Saigon Hi-Tech Park, Lot I3, N2 Street, Saigon Hi-Tech Park, District 9, Ho Chi Minh City, Vietnam.
[b)]**Author to whom correspondence should be addressed:** tien.son.nguyen@liu.se

ABSTRACT

Photo-induced current transient spectroscopy (PICTS) and electron paramagnetic resonance (EPR) are used to study irradiation-induced defects in high-purity semi-insulating (HPSI) 4H-SiC. Several deep levels with the ionization energy ranging from 0.1 to ∼1.1 eV have been observed in irradiated and annealed samples by PICTS. Among these, two deep levels, labeled E370 and E700 at ∼0.72 and ∼1.07 eV below the conduction band, respectively, are detected after high-temperature annealing. The appearance and disappearance of these two deep levels and the EPR signal of the positive C antisite–vacancy pair ($C_{Si}V_C^+$) in the sample annealed at 1000 and 1200 °C, respectively, are well correlated. Based on data from PICTS and EPR and the energies predicted by previous calculations for different charge states of dominant intrinsic defects, the E370 and E700 levels are suggested to be related to the charge transition levels (0|–) and (+|0), respectively, of the C antisite–vacancy pair. The activation energy of $E_a \sim 1.1$ eV in commercial HPSI 4H-SiC materials is, therefore, reassigned to be related to the single donor (+|0) level of $C_{Si}V_C$.

I. INTRODUCTION

Silicon carbide (SiC) is a mature wide bandgap semiconductor for high-power, high-frequency, and high-temperature devices.[1,2] In the most common polytype, 4H-SiC, intrinsic defects, including vacancies and their associated complexes, are predicted to have their different charge states located within the bandgap.[3] For most of these defects, their negative charge states locate in the upper half of the bandgap, acting as deep electron traps and have a strong influence on the electrical and optical properties of the material.

Many deep level defects have been reported in 4H-SiC by deep level transient spectroscopy (DLTS).[4,5] However, for most of them, the origin has not been identified due to difficulties in the correlation between DLTS and other experimental techniques that can provide information on the microscopic model of defects, such as electron paramagnetic resonance (EPR). Some of the charge states of vacancies and their associated complexes, such as the divacancy and antisite–vacancy pairs, are paramagnetic and can be studied by EPR. However, the combination of DLTS and EPR is difficult since DLTS probes only defects in a thin epilayer with typical concentrations in the 10^{13} cm^{-3} ranges, which is below the detection limit of EPR. Moreover, EPR measures the whole sample including the highly doped n-type substrate. This problem can be overcome using thick freestanding epilayers, which allow a direct correlation between EPR and DLTS as has been successfully used for identification of deep levels related to the C vacancy (V_C) in the single positive (V_C^+)[6] and double negative (V_C^{2-}) charge states.[6,7]

However, it requires a huge effort in growing thick epilayers (at least ~100 μm thick) and removing the substrate.

Recently, DLTS has been used in combination with photoluminescence (PL) for the identification of defects.[8,9] However, the correlation in concentration between a DLTS defect and a PL center is challenging for several reasons. DLTS defection is limited only within a thin layer while PL will detect the whole thickness of the sample, including the substrate if using below bandgap excitation. Samples used for DLTS are usually irradiated with low irradiation doses and, hence, contain low concentrations of defects (typically in the 10^{13} cm^{-3} ranges). The PL signals in such samples are usually weak, especially in the cases of proton irradiation or ion implantation when defects are mainly created at the stopping layer. Also, the PL intensity depends on the stability of the charge state of the defect, the competition between recombination channels, and the choice of excitation wavelength.

With deep levels acting as efficient carrier compensation centers, intrinsic defects have been used for the creation of high-purity semi-insulating (HPSI) SiC substrates for high-frequency power devices.[10–12] In such HPSI material with the Fermi level located near the middle of the bandgap, EPR can access different charge states of defects and has been used for the identification of intrinsic defects responsible for the SI-properties of the materials.[13] However, DLTS is not applicable for HPSI materials due to too high resistivity.

In this work, we use photo-induced current transient spectroscopy (PICTS) and EPR to study deep levels in electron-irradiated HPSI 4H-SiC. There have been several reports on PICTS observation of deep level defects in 4H-[14] and 6H-SiC.[15,16] The problem of high resistivity of irradiated HPSI materials can be overcome by measuring the photo-induced current in PICTS. With focusing on vacancy-related complexes, that require annealing at relatively high temperatures to form, we use irradiated and annealed HPSI 4H-SiC samples, in which interstitial-related defects are annealed out for reducing the overlap of signals from many deep levels in PICTS spectra. Deep level centers with the activation energy ranging from ~0.1 to ~1.1 eV in HPSI 4H-SiC samples created by irradiation and annealed at different temperatures up to 1600 °C have been observed by PICTS. The assignment of these deep levels based on PICTS and EPR data is discussed.

II. EXPERIMENTAL DETAILS

The material used in this work is commercial HPSI 4H-SiC wafers, in which the C vacancies and divacancy (V_CV_{Si}) are dominating defects.[13] The irradiation with 2 MeV electrons was performed at room temperature to a fluence of 1×10^{17} cm^{-2}. After irradiation, the wafer was cut into two sets of samples. The annealing was performed in Ar ambient at different temperatures in the range 200–1600 °C. One set of samples is used for PICTS and the other is used for EPR.

For PICTS measurements, Schottky and ohmic contacts with a diameter of 1 mm were made by evaporation of Ni and Al, respectively. The thickness of the Ni contacts is less than 10 nm, allowing the transmission of ultraviolet (UV) light excitation from a light-emitting diode (LED). Usage of the transparent Schottky contact enhances the signal-to-noise ratio of PICTS measurements.[17] The width of the UV light pulses is 10 ms.

EPR measurements were performed on a Bruker E500 X-band (~9.4 GHz) equipped with a continuous He-flow cryostat, allowing a regulation of the sample temperature from 4 to 300 K.

III. PICTS AND EPR RESULTS

A. PICTS

We notice that no clear peaks have been detected in as-irradiated samples and in samples annealed at 200 °C. This is due to a too strong background signal created by many radiation-induced defects so that the contribution to the current from individual deep levels at a certain temperature is not noticeable. The distinguished PICTS peaks appear in samples annealed at 400 °C. Figure 1 shows the PICTS spectra in irradiated samples after annealing at different temperatures (600–1600 °C) measured in the temperature range 100–400 K. The PICTS spectrum measured in the sample annealed at 400 °C is not shown since we do not observe any noticeable changes after annealing at 600 °C. For all the spectra, the current transient is analyzed using the weighting function described by Tokuda and co-workers[18] with the time constant at the peak temperature being 3.8 ms.

After annealing at 600 °C, the PICTS spectrum shows four distinguished peaks, labeled by the temperature at their maximum E150, E200, E270, and E340 and a shoulder of the strong E270 peak at ~250 K (Fig. 1). The E200 peak is too weak to be characterized. After annealing at 1000 °C, new peaks appear at 110, 160, 310, and 370 K; the E250 and E270 peaks get stronger, while the peaks E150 and E340 have either disappeared or merged with nearby stronger peaks E160 and E370, respectively. After annealing at 1200 °C, a new peak at 380 K appears while others decreases, and the E370 peaks are not seen in the spectrum. With increasing the annealing temperature to 1400 °C, the E110 and E160 peaks increase while others are reduced in intensity (E250 and E270) or disappear (E380). After annealing at 1600 °C, the E110 and E160 peaks are no longer detected and the E250 and E270 peaks are reduced further while two new peaks appear at 140 and 180 K. The activation energy E_a and the capture cross section σ_∞ of the observed PICTS peaks are given in Table I.

The above-mentioned samples were measured again in a higher-temperature range 400–750 K. Their PICTS spectra are shown in Fig. 2. Among these samples, only the sample annealed at 1000 °C shows a new peak at 700 K, labeled as E700. This peak disappears after annealing the sample at 1200 °C. Its activation energy and capture cross section are also given in Table I.

B. EPR

The EPR spectrum in an as-irradiated sample measured at 80 K for the magnetic field along the c-axis (**B**||**c**) in darkness is shown in Fig. 3. The pair of strong lines in this EPR spectrum are from the EI3 center with a spin S = 1.[19] This center is annealed out at low temperatures (~240 °C).[20] The other strong line at the center is from the positive C vacancy (V_C^+).[21] At this microwave (MW) frequency, the signals of the V_C^+ center occupying the hexagonal (*h*) and quasi-cubic (*k*) lattice sites are overlapped. The inset shows the

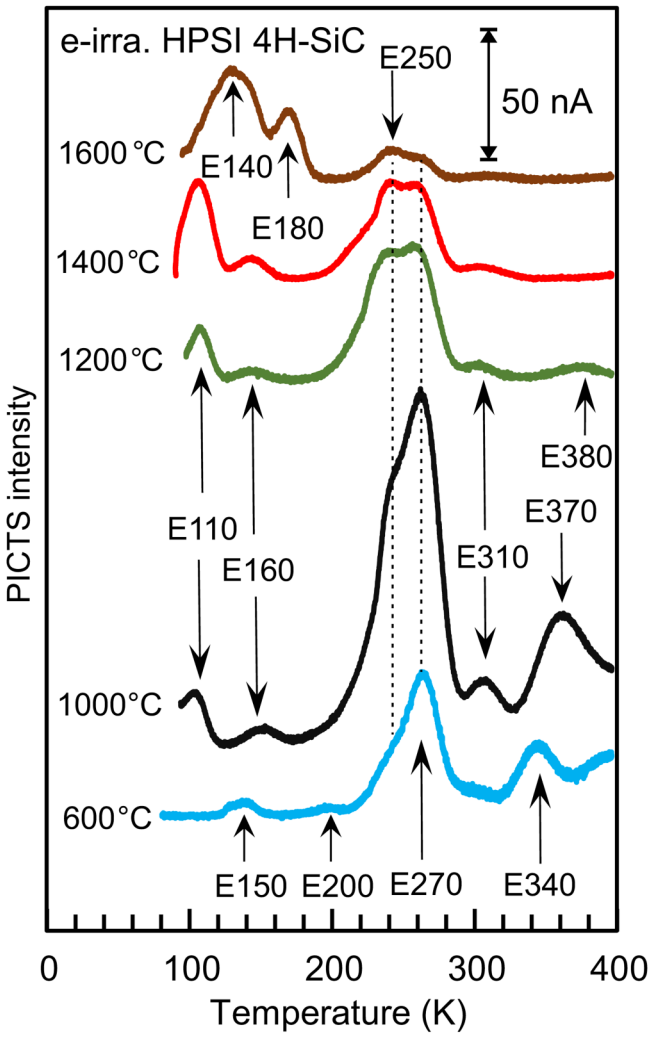

FIG. 1. PICTS spectra in HPSI 4H-SiC irradiated by 2 MeV electrons to a dose of 1×10^{17} cm^{-2} and annealed at different temperatures measured in the temperature range 100–400 K. The peaks in samples annealed at 600 °C are also detected in samples annealed at 400 °C. The current transient is analyzed using the weighting function as used in Ref. 18 with the time constant at the peak temperature for all the PICTS spectra being 3.8 ms. The sample was excited by light pulses from an UV LED (365 nm, 1 mW power).

^{29}Si hyperfine (hf) lines of $V_C^+(k)$ arisen from the interaction between the electron spin and the nuclear spin of a ^{29}Si (I = 1/2, 4.67% natural abundance) occupying one of four nearest Si neighboring of the C vacancy (the Si_1 atom along the c-axis and three equivalent Si_{2-4} atoms in the basal plane). The weak lines, labeled EI4, are related to the complex between a C antisite–vacancy pair and a C vacancy at a third neighbor of the C antisite in the neutral charge state $(V_C–C_{Si}V_C)^0$.[22] The EI4 center is already present in unirradiated HPSI materials. In addition, other four unidentified centers with spin S = 1 (indicated by arrows with different colors) are observed. The sharp and weak line close to the V_C^+ line on the high-field side is from an unidentified defect.

After annealing at 600 °C, the signals of EI3 and some other centers with spin S = 1 are annealed out while the V_C^+ signal is still dominant in the spectrum (Fig. 4). The signals of the EI4 center and other two centers with spin S = 1, one with the largest zero-field splitting (ZFS) of ∼696 G (indicated by red arrows) and the other with a ZFS of ∼180 G (indicated by green arrows), become stronger. The left inset shows the V_C^+ signal and the ^{29}Si hf structure of $V_C^+(k)$, and a weak signal of a C_{1h} configuration of the positive C antisite–vacancy pair ($C_{Si}V_C^+$) center, $C_{Si}V_C^+(hk)$.[23] With reducing the MW power by a factor of two to 1 mW, all four configurations of $C_{Si}V_C^+$ can be partly resolved as shown in the right inset of Fig. 4.

In the sample annealed at 1000 °C, the strong signal of $C_{Si}V_C^+$ is detected (Fig. 5). Two weak pairs of lines with the splitting of ∼180 and ∼333 G (indicated by green and black arrows, respectively) are from unidentified defects with spin S = 1. The signals from the V_C^+ and EI4 centers are not detected in darkness but appear under illumination (not shown). We notice that in darkness, only two configurations of the $C_{Si}V_C^+$ defect with the C vacancy occupying the hexagonal (*h*) lattice site, $C_{Si}V_C^+(hh)$ and $C_{Si}V_C^+(kh)$,[23] are observed as can be seen in the inset of Fig. 5. These two partly resolved lines are identified by their g-values and hf structures arisen from the interaction between the electron spin and the nuclear spin of one ^{29}Si occupying one of three nearest Si neighbors of the C vacancy.[23] The right inset shows the spectra of the negative Si vacancy (V_{Si}^-)[24] at inequivalent lattice sites *k* and *h* [the low- and high-field lines of $V_{Si}^-(h)$ is overlapped with the ^{29}Si hf lines of the central line of the spin S = 3/2 center[25,26]] measured at 293 K with an opposite modulation phase (90° or out phase is an optimum phase for detection of the V_{Si}^- signal). (The V_{Si}^- signal is saturated and not seen in the main spectrum since it is detected with 0° modulation phase and a high MW power of 2 mW.)

Figure 6 shows EPR spectra in samples annealed at 1200, 1400, and 1600 °C measured in darkness at 80 K for **B**||**c**. After annealing at 1200 °C, the $C_{Si}V_C^+$ signal disappears, while the signals of V_C^+ and EI4 centers reappear. A weak signal of a spin S = 1 center with the ZFS of ∼180 G (indicated by green arrows) is still observed [Fig. 6(a)]. This center is also detected in other samples annealed at lower temperatures. The V_C^+ signal decreases further but is still clearly detected after annealing at 1400 °C [Fig. 6(b)] and becomes very weak after annealing at 1600 °C [Fig. 6(c)].

IV. DISCUSSION

The EPR observation of various interstitial-related defects in as-irradiated materials suggests that there should be a significant contribution to the photocurrent in PICTS from their deep levels. A high concentration of vacancy and interstitial-related defects results in a high background photocurrent that obscures the contribution from individual deep levels. This may explain why clear peaks can only be observed by PICTS in samples annealed at temperatures ∼400 °C or higher when most of the interstitial-related defects have been annealed out.

For revealing the origin of the observed deep levels, let us first compare the PICTS data with previously reported results. Since

TABLE I. The activation energy and capture cross section of deep levels observed by PICTS in irradiated and annealed HPSI 4H-SiC. Some of the peaks show a large uncertainty in the activation energy and capture cross section due to overlapping with other signals.

PICTS peak	Annealing range (°C)	E_a (eV)	σ_∞ (cm^2)	Assignment
E110	1000–1400	0.11–0.22	1×10^{-17}–4×10^{-13}	Ti[5,43]
E140	1600	0.13	3×10^{-18}	Ti[5,43]
E150	200–600	0.2–0.3	9×10^{-17}–1×10^{-13}	S1[8,28]
E160	1000–1600	0.35	9×10^{-11}	B[38,39]
E180	1600	0.40	1×10^{-10}	HS1[41]
E250	400–1600	0.44	9×10^{-12}	D-center[39,40]
E270	400–1600	0.6–0.7	5×10^{-12}–5×10^{-10}	Z1/2[5,7]
E310	800–1400	0.5–0.6	5×10^{-16}–7×10^{-14}	
E340	200–800	0.7–0.9	4×10^{-13}–7×10^{-11}	S2, EH4[4,8,28]
E370	1000	0.72	1×10^{-13}	$C_{Si}V_C^-$
E380	1200	0.81	5×10^{-13}	
E700	1000	1.07	1×10^{-16}	$C_{Si}V_C^0$

PICTS cannot distinguish the emission to the conduction or the valence band from deep levels, our assignment of the observed peaks to the previously reported DLTS levels is based on the activation energy E_a in both n- and p-type materials and their thermal stability.

From the obtained activation energy of $\sim E_a$ – (0.6–0.7) eV and the thermal stability, the E270 peak can be identified as the Z1/2 centers [at $\sim E_C$ – (0.63–0.68) eV],[5] which are related to the double acceptor level of the C vacancy, V_C^{2-}, at two inequivalent lattice sites.[6,7,27] The EPR data also show the presence of V_C in all irradiated and annealed samples with the same trend of reducing concentration with increasing annealing temperature as seen for the E270 peak.

The PICTS spectrum in samples annealed at 600 °C is indeed very similar to the DLTS spectrum in irradiated 4H-SiC epilayers reported by David and co-workers,[28] which also contain the Z1/2 center and lower- and higher-temperature peaks (S1 and S2, respectively). The S1 and S2 levels were recently assigned to the triple and double negative charge states, respectively, of the Si vacancy in a recent study, which combines data from DLTS, photoluminescence (PL), and density functional theory (DFT) calculations.[8] The activation energies of the peak E150 ($\sim E_C$ – 0.3 eV) and E310 [$\sim E_C$ – (0.5–0.6 eV)] are close to that of the S1 ($\sim E_C$ – 0.4 eV) and S2 ($\sim E_C$ – 0.7 eV) centers,[28] respectively. After annealing at 1000 °C, the EPR signal of the Si vacancy is still detected but much weak (Fig. 5), while in PICTS, the E310 peak increases (Fig. 1). This may suggest that if the E150 and E310 peaks are related to S1 and S2, respectively, then the E310 peak is likely contributed also from another defect that appears after annealing at 1000 °C. Considering the ionization energy, the E340 peak at $\sim E_C$ – (0.7–0.9) eV may also be related to the S2 level or the EH4 level (at $\sim E_C$ – 0.72 eV[4] or $\sim E_C$ – 1.0 eV).[9,29]

The activation energy ($E_a \sim 1.07$ eV) of the E700 peak is close to the (+|0) donor level of the $C_{Si}V_C$ center at $\sim E_C$ – 1.1 eV as predicted by DFT calculations[30,31] and determined by photoexcitation-EPR.[32] For E370 peak, its activation energy ($E_a \sim 0.72$ eV) is close to the (0|–) acceptor level of $C_{Si}V_C$ predicted by calculations at $\sim E_C$ – (0.4–0.6) eV.[30,31] Moreover, the appearance and disappearance of these two PICTS peaks and the EPR signal of $C_{Si}V_C^+$ in the sample annealed at 1000 and 1200 °C, respectively, are well correlated, supporting the assignment of the E370 and E700 peaks to the (0|–) and (+|0) levels, respectively, of $C_{Si}V_C$. The absence of the E700 peak in the sample annealed at 600 °C, in which the $C_{Si}V_C^+$ center has already been observed by EPR, as shown in the right inset of Fig. 4, may be due to inappropriate Fermi level. For considering the effect of the Fermi level on PICTS, let us find out where the Fermi level locates in the as-irradiated sample and how it changes with annealing temperature.

It is known that the (+|0) single donor level of the C vacancy at $\sim E_C$ – 1.5 eV[6,33] is very close to its (2+|+) double donor level [$\sim E_C$ – (1.6–1.7) eV].[30,33] This means that the C vacancy can be in the single positive charge state in equilibrium only if the Fermi level locates at the (2+|+) level or between its (2+|+) and (+|0) levels. This occurs in HPSI 4H-SiC materials grown by PVT that have an activation energy of $E_a \sim 1.5$ eV.[11,12] Such a material is "p-type like" with a higher concentration of residual acceptors (the concentration of residual boron acceptor is higher than that of the residual N donor, [B] > [N]), which is then compensated by the donor levels of the C vacancy at $\sim E_C$ – 1.5 eV.

The observation of the V_C^+ signal in darkness in the as-irradiated sample and in the sample annealed at 600 °C indicates that the Fermi level locates at the donor levels of V_C. Although the (+|0) donor level of $C_{Si}V_C$ (at $\sim E_C$ – 1.1 eV) lies higher than the donor levels of V_C, its concentration is still not enough to compensate the B acceptor and the lower-lying acceptor (0|–) of V_{Si} (at $\sim E_C$ – 1.25 eV).[30,31] Therefore, the donor levels of V_C in the carrier compensation process, pinning the Fermi level at its donor levels. This ensures that the $C_{Si}V_C$, whose (2+|+) level locates at $\sim E_V$ + (1.3–1.4) eV or $\sim E_C$ – (1.9–2.0) eV,[30,31] is stable in the single positive charge state as confirmed by the EPR observation of all four configurations of $C_{Si}V_C^+$ in darkness (Fig. 4). The (2+|+) donor level of $C_{Si}V_C$ is too deep to prober by PICTS in the studied temperature range. Its (+|0) level is a donor level and not an electron trap and, hence, will not be detected by PICTS if the Fermi level locates well below. This explains the absence of the E700 peak in the sample annealed at 600 °C.

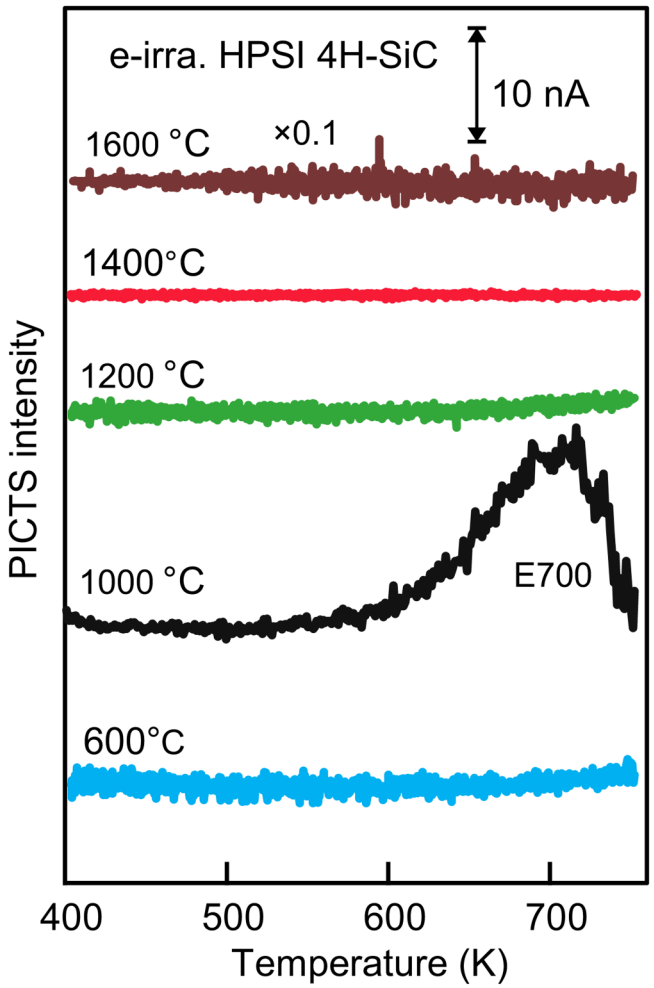

FIG. 2. PICTS spectra in HPSI 4H-SiC irradiated by 2 MeV electrons to a dose of 1×10^{17} cm^{-2} and annealed at different temperatures measured in the temperature range 400–750 K. The spectrum in the sample annealed at 1600 °C is shown in a 1/10 scale. The sample was excited by light pulses from an UV LED (375 nm, 15 mW power).

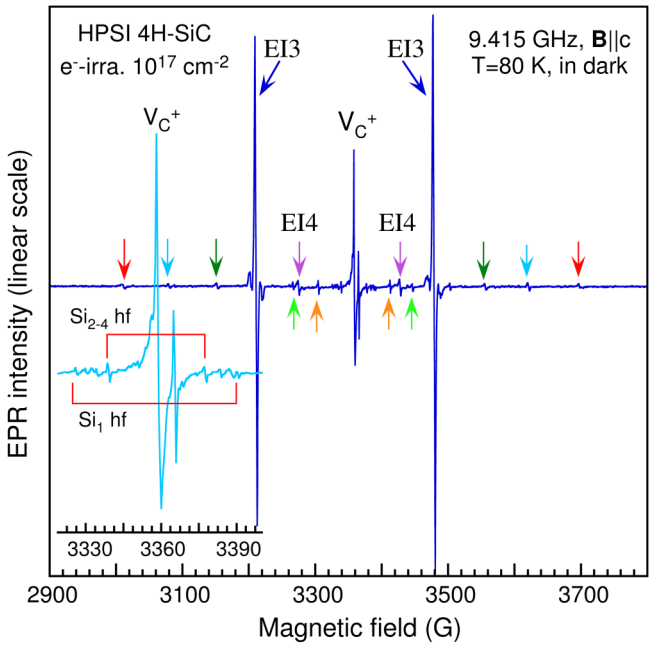

FIG. 3. EPR spectrum in as-irradiated HPSI 4H-SiC measured for the magnetic field along the c-axis (**B||c**) in darkness, showing the dominant signals from the EI3 center[19] and the positive C vacancy V_C^+. The weak signal EI4 is from a V_C-related complex,[22] which already present in as-grown HPSI materials. Five other weak pairs of lines (indicated by arrows with different colors) are from unidentified centers with spin S = 1. The inset shows the V_C^+ signal and the ^{29}Si hf structure of $V_C^+(k)$ in an extended magnetic field scale. The sharp and weak line close to the V_C^+ line on the high-field side is from an unidentified defect.

After annealing at 1000 °C, the concentration of $C_{Si}V_C$ pair increases and its (+|0) donor level at ~E_C–1.1 eV can compensate the B acceptor, the Si vacancy, and the lower-lying (0|–) and (–|2–) acceptor levels of the divacancy ($V_{Si}V_C$) (at ~1.3 and ~1.2 eV, respectively,[34]) pinning the Fermi level at its (+|0) donor level. The configurations of $C_{Si}V_C$ with higher (+|0) levels will become positively charged ($C_{Si}V_C^+$), while other configurations with deeper (+|0) levels may remain in the neutral charge state. This explains why only two configurations $C_{Si}V_C^+(hh)$ and $C_{Si}V_C^+(kh)$ are detected by EPR in darkness (Fig. 5). This location of the Fermi level transforms V_C^+ to V_C^0 and $V_{Si}V_C^0$ to $V_{Si}V_C^{2-}$, explaining the absence of the EPR signals of V_C^+ and the neutral divacancy $V_{Si}V_C^0$[35] in the sample annealed at 1000 °C. The neutral charge state of $C_{Si}V_C$ and its higher lying (0|–) acceptor state, which is an electron trap, will contribute to photocurrent, leading to the observation of the E370 and E700 levels in PICTS. This also suggests that the (+|0) donor level of $C_{Si}V_C$ is responsible for the semi-insulating properties of HPSI 4H-SiC materials with an activation energy $E_a \sim 1.1$ eV, which was previously assigned to acceptor levels of either V_C or $C_{Si}V_C$.[13]

After annealing at 1200 °C, the concentration of $C_{Si}V_C$ is reduced and can no longer compensate the B acceptor. The C vacancy then involves in the carrier compensation process and compensates the rest of B to pull the Fermi level back to its donor levels, transforming V_C^0 to V_C^+. This explains the reappearance of the V_C^+ signal in the EPR spectrum.

In a previous PICTS study of as-grown semi-insulating 4H-SiC,[14] a deep level (SN6) with an activation energy of ~1.16 eV has been observed. After neutron irradiation, it appears as a weak shoulder of other stronger signals. The SN6 deep level was assigned to the EH5 level[4] and attributed to the divacancy.[14] In a recent study by Karsthof and co-workers,[9] two previously reported DLTS levels EH4 and EH5[4] were assigned to a PL band in the spectral region of 640–680 nm, which was attributed to the $C_{Si}V_C^0$ center by Steeds.[36] In that study,[9] the EH4 level (at ~E_C–0.72 eV[4]) was redetermined to be at ~E_C–1.0 eV, and both EH4 and EH5 (at ~E_C–1.13 eV[4]) were assigned to the (+|0) level of different configurations of $C_{Si}V_C$.

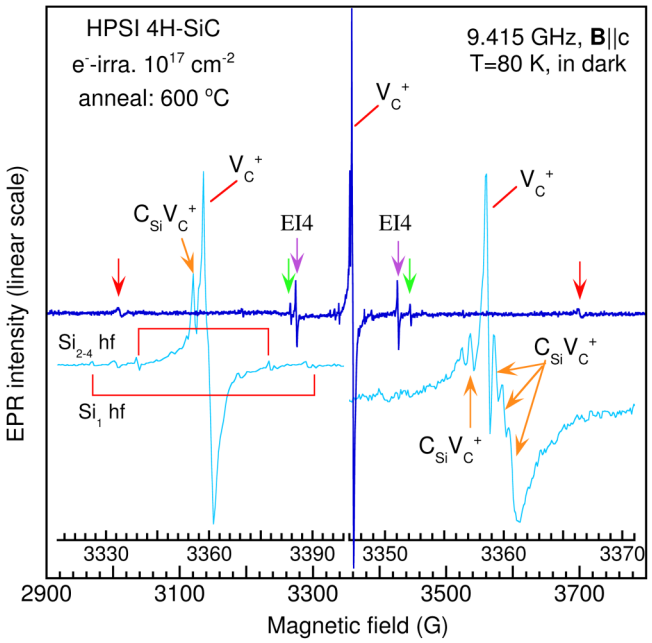

FIG. 4. EPR spectrum in irradiated HPSI 4H-SiC after annealing at 600 °C measured at 80 K for **B**||**c** in darkness. The V_C^+ line is still dominant in the spectrum showing a strong signal of the positive C vacancy V_C^+.[21] The EI4 lines and two pairs of lines, one with the largest splitting of ∼696 G (indicated by red arrows) and the other with a splitting of ∼180 G (indicated by green arrows) in the as-irradiated sample in Fig. 3 become stronger. The left inset shows the V_C^+ line and the ^{29}Si hf structure of $V_C^+(k)$. With reducing the MW power by a factor of two to 1 mW and increasing the field resolution (∼10 data points/G), partly resolved lines from the four configurations of the $C_{Si}V_C^+$ center can be seen as shown in the right inset.

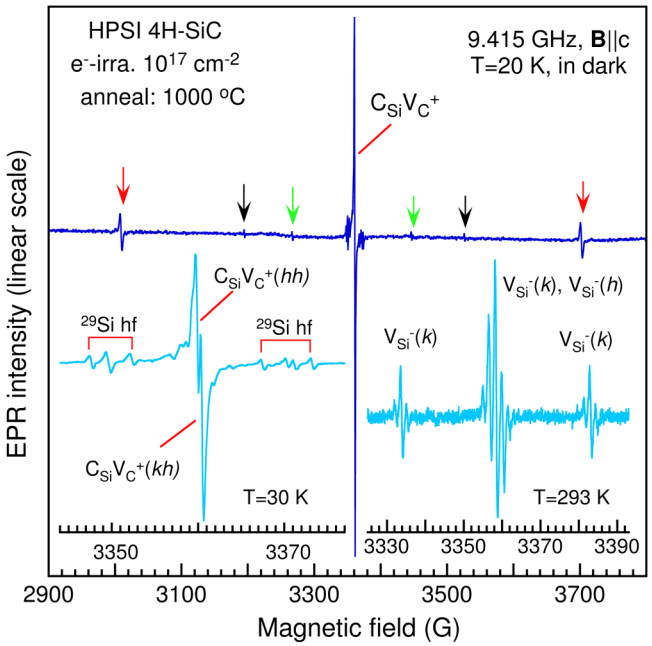

FIG. 5. EPR spectrum in irradiated HPSI 4H-SiC after annealing at 1000 °C measured at 20 K for **B**||**c** in darkness, showing a strong signal of the positive C antisite–vacancy pair $C_{Si}V_C^+$.[23] The pair of lines with the largest splitting (∼696 G) in as-irradiated sample in Fig. 3 becomes stronger (indicated by arrows). The left inset shows the central part of the spectrum measured at 30 K with a higher field resolution (∼10 data points/G), where two partly resolved lines from the (*hh*) and (*kh*) configurations of $C_{Si}V_C^+$ and their ^{29}Si hf lines can be seen. The right inset shows the V_{Si}^- center[24] measured at 293 K in darkness with an opposite modulation phase (90°), a lower MW power (0.6325 mW), and a lower field modulation (0.6 G).

The EH4 and EH5 DLTS levels are different from the E700 level that we observed by PICTS, although they have a similar ionization energy. The concentration of the EH4 and EH5 centers is found to be highest in as-irradiated samples and it decreases with increasing annealing temperatures in the range 20–1000 °C.[9] The annealing behavior of EH4 and EH5 is unexpected for a V_{Si}-related complex defect as $C_{Si}V_C$. Theoretical calculations predict barriers between 3.6 and 4.3 eV for transformation from V_{Si} to $C_{Si}V_C$ and this process may not occur at temperatures lower than ∼600 °C.[31] EPR studies also confirm that the V_{Si}^- center does not change in intensity in the annealing temperature range 20–600 °C.[26] Moreover, EH4 is observed only in samples irradiated with high-energy electrons while EH5 is a metastable defect and can be created by low-energy (200 keV) electron irradiation, which can only displace C atoms and creates C vacancies and C interstitials.[37] Therefore, the assignment of the DLTS levels EH4 and EH5 to the (+|0) level of different configurations of $C_{Si}V_C$ by Karsthof and co-workers[9] is questionable.

Now we consider possible origins of deep levels with smaller activation energies and stable at high temperatures: E110-E250.

Boron is a shallow acceptor in SiC with an activation energy of ∼0.29–0.39 eV.[38,39] It is known to be present in HPSI 4H-SiC materials with a concentration in the low 10^{15} cm^{-3} range.[10–12] In samples irradiated to a fluence of 1×10^{17} cm^{-2}, the B concentration should be an order of magnitude lower compared to the concentration of primary intrinsic defects. Its contribution to the current in PICTS may not be seen in the strong background current. However, in samples annealed at high temperatures when interstitials and vacancies are annealed out or formed complexes, B is expected to be seen in PICTS. We suggest that the E160 peak with an activation energy of 0.35 eV observed in samples annealed at 1000 °C and higher temperatures is related to the shallow boron acceptor.

The D center[39]—a complex of boron with a C vacancy—is expected to be present in irradiated and annealed HPSI 4H-SiC samples. Its activation energy ($E_a \sim 0.47$ eV[40]) is close to that of the E250 peak ($E_a \sim 0.44$ eV). The high thermal stability of the E250 peak is also expected for this complex defect.[40] We, therefore, assign the E250 peak to the D center.

The E180 peak is among a few defect levels that are stable at 1600 °C. With the activation energy $E_a \sim 0.4$ eV and such thermal stability, the E180 peak may be related to the HS1 donor level at $E_V + 0.35$ eV,[41] which was suggested to be related to the Si antisite Si_C.[42]

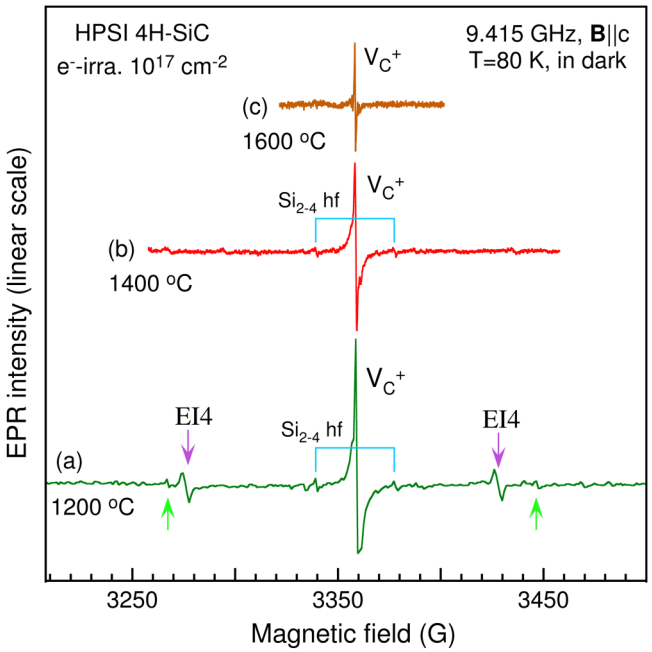

FIG. 6. EPR spectra in irradiated HPSI 4H-SiC after annealing at 1200, 1400, and 1600 °C, measured in darkness at 80 K for **B||c**. (a) After annealing at 1200 °C, the $C_{Si}V_C^+$ signal disappears while the signals of the V_C^+ and EI4 centers are observed again. The spin S = 1 center with a ZFS of ∼180 G is still detected (indicated by green arrows). The signal of V_C^+ is reduced but their ^{29}Si hf lines are still detected. After annealing at (b) 1400 and (c) 1600 °C, the V_C^+ signal decreases further but is still detected. Other S = 1 centers are not detectable after annealing at 1600 °C.

The E110 and E140 peaks are very thermally stable and have very small activation energies ($E_a \sim 0.11$–0.22 eV). Theoretical calculations predict no intrinsic defects having states that are close to the band edges. The involvement of impurities in these levels may be more likely. Titanium (Ti) is present in HPSI 4H-SiC materials with a concentration of 10^{14} cm^{-3}.[10–12] Titanium has acceptor levels at $\sim E_C - (0.11$–$0.13)$ and $\sim E_C - (0.15$–$0.17)$ eV for the substitutional Ti center at the hexagonal and quasi-cubic lattice sites, respectively.[5,43] The E110 and E140 peaks are, therefore, attributed to acceptor levels of the substitutional Ti.

In the PICTS study by Naval and co-workers,[14] two levels, SN2b ($E_a \sim 0.49$ eV) and SN5 ($E_a \sim 0.81$ eV), have been reported. Their activation energies are close to that of the E310 and E380 peaks, respectively. However, both the SN2b and SN5 levels are observed in as-irradiated samples, while E310 and E380 peaks could only be detected after high-temperature annealing. Therefore, for E310 and E380 peaks, more data are needed for the identification of their origin.

V. SUMMARY

In summary, we have observed several defect levels in irradiated HPSI 4H-SiC by PICTS. EPR studies on the same material reveal vacancies, divacancies, and C vacancy–antisite pairs as dominating defects in samples annealed at different temperatures. Based on the data from PICTS and EPR in annealing studies, the deep levels E370 and E700 are assigned to the charge transition levels (0|–) and (+|0) of the C antisite–vacancy pair, respectively. Our result suggests that the (+|0) donor level of the $C_{Si}V_C$ center at $\sim E_C - 1.07$ eV is responsible for the semi-insulating properties of HPSI 4H-SiC materials with an activation energy of $E_a \sim 1.1$ eV, which was previously attributed to either the single acceptor (0|–) level of V_C or the (1–|2–) level of $C_{Si}V_C$.[13] With the annealing of the $C_{Si}V_C$ center at 1200 °C and the stability of the C vacancy at 1600 °C as observed in our experiments, we reassign the change of the activation energy in HPSI 4H-SiC materials after annealing at 1600 °C from ∼1.1 to ∼0.6 eV as observed in Ref. 13 to the shift of the Fermi level from the (+|0) donor level of $C_{Si}V_C$ (at $\sim E_C$–1.07 eV) to the (2–) double acceptor level of V_C at $\sim E_C$–0.68 eV when the $C_{Si}V_C$ pair being annealed out.

ACKNOWLEDGMENTS

Financial support by the Grant-in-Aid for Scientific Research Grant No. 25390067 for H.N., M.K., and Y.O., the Swedish Research Council (Grant No. VR 2016-05362 for I.G.I. and No. VR 2016-04068 for N.T.S.), the EU H2020 project QuanTELCO (Grant No. 862721), and the Knut and Alice Wallenberg Foundation (Grant No. KAW 2018.0071) for N.T.S. and I.G.I. is acknowledged. T.O. thanks the Japan Society for the Promotion of Science Grant Nos. JSPS KAKENHI 20H00355 and 18H03770.

DATA AVAILABILITY

The data that support the findings of this study are available from the corresponding author upon reasonable request.

REFERENCES

[1]H. Matsunami and T. Kimoto, Mater. Sci. Eng. R **20**, 125 (1997).
[2]J. A. Cooper, M. R. Melloch, R. Singh, A. Agarwal, and J. W. Palmour, IEEE Trans. Electron Devices **49**, 658 (2002).
[3]L. Torpo, M. Marlo, T. E. M. Staab, and R. M. Nieminen, J. Phys.: Condens. Matter **13**, 6203 (2001).
[4]C. Hemmingsson, N. T. Son, O. Kordina, J. P. Bergman, E. Janzén, J. L. Lindström, S. Savage, and N. Nordell, J. Appl. Phys. **81**, 6155 (1997).
[5]T. Dalibor, G. Pensl, H. Matsunami, T. Kimoto, W. J. Choyke, A. Schöner, and N. Nordell, Phys. Status Solidi A **162**, 199 (1997).
[6]N. T. Son, X. T. Trinh, L. S. Løvlie, B. G. Svensson, K. Kawahara, J. Suda, T. Kimoto, T. Umeda, J. Isoya, T. Makino, T. Ohshima, and E. Janzén, Phys. Rev. Lett. **109**, 187603 (2012).
[7]K. Kawahara, X. Thang Trinh, N. Tien Son, E. Janzén, J. Suda, and T. Kimoto, Appl. Phys. Lett. **102**, 112106 (2013).
[8]M. E. Bathen, A. Galeckas, J. Müting, H. M. Ayedh, U. Grossner, J. Coutinho, Y. K. Frodason, and L. Vines, npj Quantum Inf. **5**, 111 (2019).
[9]R. Karsthof, M. E. Bathen, A. Galeckas, and L. Vines, Phys. Rev. B **102**, 184111 (2020).
[10]A. Ellison, B. Magnusson, N. T. Son, L. Storasta, and E. Janzén, Mater. Sci. Forum **433–436**, 33 (2003).
[11]S. G. Müller, M. F. Brady, W. H. Brixius, R. C. Glass, H. McD Hobgood, J. R. Jenny, R. T. Leonard, D. P. Malta, A. R. Powell, V. F. Tsvetkov, S. T. Allen, J. W. Palmour, and C. H. Carter, Jr., Mater. Sci. Forum **433–436**, 39 (2003).

[12]J. R. Jenny, D. P. Malta, M. R. Calus, S. G. Müller, A. R. Powell, V. F. Tsvetkov, H. McD Hobgood, R. C. Glass, and C. H. Carter, Jr., Mater. Sci. Forum **457–460**, 35 (2004).
[13]N. T. Son, P. Carlsson, J. ul Hassan, B. Magnusson, and E. Janzén, Phys. Rev. B **75**, 155204 (2007).
[14]F. Nava, A. Castaldini, A. Cavallini, P. Errani, and V. Cindro, IEEE Trans. Nucl. Sci. **53**, 2977 (2006).
[15]M. Kato, K. Kito, and M. Ichimura, J. Appl. Phys. **108**, 053718 (2010).
[16]B. Berger, N. Schüler, S. Anger, B. Gründig-Wendrock, J. R. Niklas, and K. Dornich, Phys. Status Solidi A **208**, 769 (2011).
[17]P. Blood and J. W. Orton, *The Electrical Characterization of Semiconductors: Majority Carriers and Electron States* (Academic Press Ltd., London, 1992).
[18]Y. Tokuda, N. Shimizu, and A. Usami, J. Appl. Phys. **18**, 309 (1979).
[19]N. T. Son, W. M. Chen, J. L. Lindström, B. Monemar, and E. Janzén, Mater. Sci. Eng. B **61–62**, 202 (1999).
[20]N. T. Son, P. N. Hai, and E. Janzén, Mater. Sci. Forum **353–356**, 499 (2001).
[21]N. T. Son, P. N. Hai, and E. Janzén, Phys. Rev. B **63**, 201201(R) (2001).
[22]P. Carlsson, N. T. Son, A. Gali, J. Isoya, N. Morishita, T. Ohshima, B. Magnusson, and E. Janzén, Phys. Rev. B **82**, 235203 (2010).
[23]T. Umeda, J. Isoya, T. Ohshima, N. Morishita, H. Itoh, and A. Gali, Phys. Rev. B **75**, 245202 (2007).
[24]N. Mizuochi, S. Yamasaki, H. Takizawa, N. Morishita, T. Ohshima, H. Itoh, and J. Isoya, Phys. Rev. B **66**, 235202 (2002).
[25]V. Ivády, J. Davidsson, N. T. Son, T. Ohshima, I. A. Abrikosov, and A. Gali, Phys. Rev. B **96**, 161114 (2017).
[26]N. T. Son, P. Stenberg, V. Jokubavicius, H. Abe, T. Ohshima, J. Ul Hassan, and I. G. Ivanov, J. Phys.: Condens. Matter **31**, 195501 (2019).
[27]X. T. Trinh, K. Szász, T. Hornos, K. Kawahara, J. Suda, T. Kimoto, A. Gali, E. Janzén, and N. T. Son, Phys. Rev. B **88**, 235209 (2013).
[28]M. L. David, G. Alfieri, E. M. Monakhov, A. Hallén, C. Blanchard, B. G. Svensson, and J. F. Barbot, J. Appl. Phys. **95**, 4728 (2004).
[29]G. Alfieri, E. V. Monakhov, B. G. Svensson, and M. K. Linnarsson, J. Appl. Phys. **98**, 043518 (2005).
[30]K. Szász, V. Ivády, I. A. Abrikosov, E. Janzén, M. Bockstedte, and A. Gali, Phys. Rev. B **91**, 121201(R) (2015).
[31]J. Coutinho, Crystals **11**, 167 (2021).
[32]N. T. Son, P. Stenberg, V. Jokubavicius, H. Abe, T. Ohshima, J. Ul Hassan, and I. G. Ivanov, Appl. Phys. Lett. **114**, 212105 (2019).
[33]I. D. Booker, E. Janzén, N. T. Son, J. Hassan, P. Stenberg, and E. Ö. Sveinbjörnsson, J. Appl. Phys. **119**, 235703 (2016).
[34]B. Magnusson, N. T. Son, A. Csore, A. Gällström, T. Ohshima, A. Gali, and I. G. Ivanov, Phys. Rev. B **98**, 195202 (2018).
[35]N. T. Son, P. Carlsson, J. Ul Hassan, E. Janzén, T. Umeda, J. Isoya, A. Gali, M. Bockstedte, N. Morishita, T. Ohshima, and H. Itoh, Phys. Rev. Lett. **96**, 055501 (2006).
[36]J. W. Steeds, Phys. Rev. B **80**, 245202 (2009).
[37]F. C. Bayer, C. G. Hemmingsson, H. Pedersen, A. Henry, J. Isoya, N. Morishita, T. Ohshima, and E. Janzén, J. Phys. D: Appl. Phys. **45**, 455301 (2012).
[38]T. Troffer, M. Schadt, T. Frank, H. Itoh, G. Pensl, J. Heindl, H. P. Strunk, and M. Maier, Phys. Status Solidi A **162**, 277 (1997).
[39]T. Stiasny and R. Helbig, Inst. Phys. Conf. Ser. **142**, 389 (1996).
[40]Y. Negoro, T. Kimoto, and H. Matsunami, J. Appl. Phys. **98**, 043709 (2005).
[41]L. Storasta, F. Carlsson, S. Sridhara, J. Bergman, A. Henry, T. Egilsson, A. Hallen, and E. Janzen, Appl. Phys. Lett. **78**, 46 (2001).
[42]T. A. G. Eberlein, R. Jones, S. Öberg, and P. R. Briddon, Phys. Rev. B **74**, 144106 (2006).
[43]N. Achtziger and W. Witthuhn, Appl. Phys. Lett. **71**, 110 (1997).